UDC 532.22:532.528

# WATER IMPACT OF AN EXPANDING CYLINDRICAL BODY

**Yu. N. Savchenko, Yu. A. Semenov, O. I. Naumova**

*Institute of Hydromechanics of NAS of Ukraine*
*Zhelyabov Str., 8/4, 03057, Kyiv, Ukraine*
†*E-mail: vnsvns60@gmail.com*

*Received 03.03.2016*

A self-similar flow with the splash jet generated by water entry of an expanding two-dimensional arbitrarily shaped body is studied theoretically based on the incompressible velocity potential theory. The flow is assumed to be irrotational, the liquid to be ideal, and gravity and surface tension are ignored. The solution is obtained in the form of integral equations using the integral hodograph method. It is shown the solution with the detached splash jet exists in all ranges of expansion speeds from zero to infinity. Detailed results in terms of pressure distribution, free surface shape and streamlines, and contact angle of the splash jet are presented.

*KEY WORDS: water entry, free surface flow, splash jet*

## 1. INTRODUCTION

The similarity solutions play an important role in fluid mechanics. When a self-similar solution exists, it enables variables in the governing equations to be combined into new ones, and the number of variables is reduced as a result. It becomes particularly effective when a partial differential equation becomes an ordinary one or an unsteady problem becomes steady in the self similar variables. In some cases, such a transformation allows an explicit form of the solution of the problem to be obtained, or the solution procedure to be significantly simplified. The result can then provide some real insights into the physics of the problem.

For the liquid/structure impact problem, its mathematical modelling is very challenging due to rapid changes of the free-surface shape and velocity in local areas, together with high speed jets. The pioneering works on water impact problem based on impulse solution for a plate were carried out by von Karman [1] and Wagner [2]. The complete linearized solution of the water entry of a wedge was first proposed by Mackie [3]. Garabedian [4,5], extensively studied main properties of the water-entry flows, including existence and uniqueness of the similarity solutions and the limit of the contact angle between the free surface and the wedge.

Remarkable progress in the understanding of fluid/structure and fluid/fluid impact phenomena has been achieved over the last decades, which has been based on further development of Wanger's theory together with the technique of matched asymptotic expansions

(Armand and Cointe [6], Howison et al. [7], Korobkin [8]). Different simplified models for the wedge entry problem have been also proposed by Greenhow [9], and Mei et al. [10].

In general, the water-entry processes are fully transient, and the temporal and spatial variables are fully independent. However, in some cases, especially at initial stage of impact and/or in some local areas, the flow may be treated as self similar, which simplifies the analysis and gives some insight into the flow topology during the impacts. Examples include those by Cumberbatch [11] for a liquid wedge impacting on a flat wall, Dobrovolskaya [12] and Zhao and Faltinsen [13] for a symmetric solid wedge entering a calm water surface, Semenov and Iafrati [14] for water entry of an asymmetric wedge, Semenov et al. [15] for an impact between two liquids of the same density, Iafrati and Korobkin [16] for flow near the corner of a horizontal plate impacting a flat surface at the initial stage.

The problem of the expanding body entering the free surface has another physical implications. One of the practical problems is the wave flow generated by a fast ship, in which the so called $2D + t$ method has been both used in the simulation (Faltinsen [17]) and in the experiment (Shakeri et al. [18]). In such a method, the flow at each transverse section is considered as two-dimensional (2D). As the section under consideration moves along the ship length from the bow, it effectively expands. For a fast ship with shaped sections, the problem becomes that of an expanding body considered here. Similar problem arises during ditching of an aircraft, that is an emergency condition that ends with the planned impact of the aircraft with water (Climent et al. [19]).

In this study we consider the nonlinear self-similar problem of the cylindrical body entering the undisturbed flat free surface. In particular, the results in section 3 are presented for a circular cylinder. The radius of the cylinder expands at a speed that is in a fixed ratio to the entry speed. The integral hodograph method (Semenov and Cummings [20]) is used to derive analytical expressions for the complex velocity, for the complex potential and mapping function, all defined in a parametric plane for which the first quadrant is chosen. It enables the original partial differential equation with nonlinear boundary conditions on the unknown free surface to be reduced to a system of integro-differential equations along straight lines in the parametric plane. The coupled equations are then solved through successive approximations. The solution contain one free parameter $b$, which determines the speed of expansion of the body. As $b \to 0$, the expansion speed of the body and the velocity at the tip of the splash approach infinity. However, at $b = 0$ the singularity in the mapping function corresponding to the tip of the splash jet disappears and the solution corresponds to the splash jet attached to the body.

The results are provided through the streamlines, free surface shape and pressure distributions along the wetted surface of the cylinder in the wide range of expansion speeds.

## 2. FORMULATION OF THE PROBLEM AND THE SOLUTION METHODOLOGY

We consider an arbitrary shaped body which expands in time in a self-similar way during its entry into a liquid of infinite depth at constant vertical velocity $V$. The liquid is assumed to be inviscid and incompressible, the flow is irrotational, gravity and surface tension are ignored. The flow region in the physical complex plane $Z = X + iY$, which boundary consists of the wetted part of the body and the free surface, can be written through

that in the stationary, or similarity plane $z = x + iy$ in terms of the self-similar variables $x = X/(Vt), y = Y/(Vt)$:

$$Z(S,t) = Vtz(s), \tag{1}$$

where $t$ is the time, $S$ and $s = S/(Vt)$ are the arc length coordinates in the physical and stationary planes, respectively.

The complex-velocity potential $W(Z,t)$ for the self-similar flow can be written as

$$W(Z,t) = \Phi(Z,t) + i\Psi(Z,t) = V^2 t w(z) = V^2 t[\varphi(z) + i\psi(z)], \tag{2}$$

where $\phi$ and $\psi$ are the velocity potential and the stream function in the similarity plane.

The problem is to determine the function $w(z)$ which conformally maps the similarity plane $z$ onto the complex-velocity potential region $w$. For solving the problem we use hodograph method and introduce a parameter plane $\zeta$ as suggested by Joukovskii [21] and Michel [22]. Instead of function $w(z)$, they proposed to find two complex functions both defined in the $\zeta$ is plane, which are the complex velocity, $dw/dz$, and the derivative of the complex potential, $dw/d\zeta$. Once these functions are found, the relation between the parameter and stationary planes can be determined as follows:

$$z(\zeta) = z_0 + \int_0^\zeta \frac{dz}{d\zeta} d\zeta = z_0 + \int_0^\zeta \frac{dw/d\zeta}{dw/dz} d\zeta, \tag{3}$$

where $z_0 = z(\zeta)_{\zeta=0}$.

As suggested by Gurevich [23] we chose the first quadrant of the $\zeta$-plane shown in (Fig. 1b) as the parameter region which corresponds to the flow region in the stationary plane in (Fig. 1a). The origin of the Cartesian system of coordinates $xy$ is chosen at the bottom point of the body as shown in (Fig. 1a). The half space of the liquid with the flat undisturbed free surface moves with constant velocity $V$ along $y$-axis and impacts the body at time instant $t = 0$. The flow is symmetric respect to $y$-axis, therefore, we can consider only right hand side of the flow region. At the instant of impact points $A, O, B$ coincide with the origin. Immediately after the impact $t > 0$, the flow topology changes. The splash jet $O, B$ with its tip angle $\mu$ at point $B$ and point $O$ of flow detachment are appear.

The functions $dw/dz$ and $dw/d\zeta$ conformally map the parameter region onto the regions of the complex velocity and the derivative of the complex potential. The basic theorem on conformal mapping allows us to fix three arbitrary points in the parameter plane, which are chosen as $OD$ (a point at infinity) and $A$, as shown in (Fig. 1b). In this plane, the interval $0 < \eta < b$ of the imaginary axis corresponds to the splash jet $OB$ and the interval $b < \eta < \infty$ corresponds to the main free surface $BD$. The interval $0 < \eta < 1$ of the real axis corresponds to the wetted part of the body, and the rest of the positive real axis ($1 < \eta < \infty$) corresponds to the symmetry line $AD$. The point $\zeta = ib$ in (Fig. 1b) is the image of the tip of the splash jet in the similarity plane (point $B$). The parameter $b$ is unknown and have to be determined from the solution. In order to determine the functions $dw/dz$ and $dw/d\zeta$ we shall formulate appropriate boundary-value problems for each of them in the $\zeta$-plane.

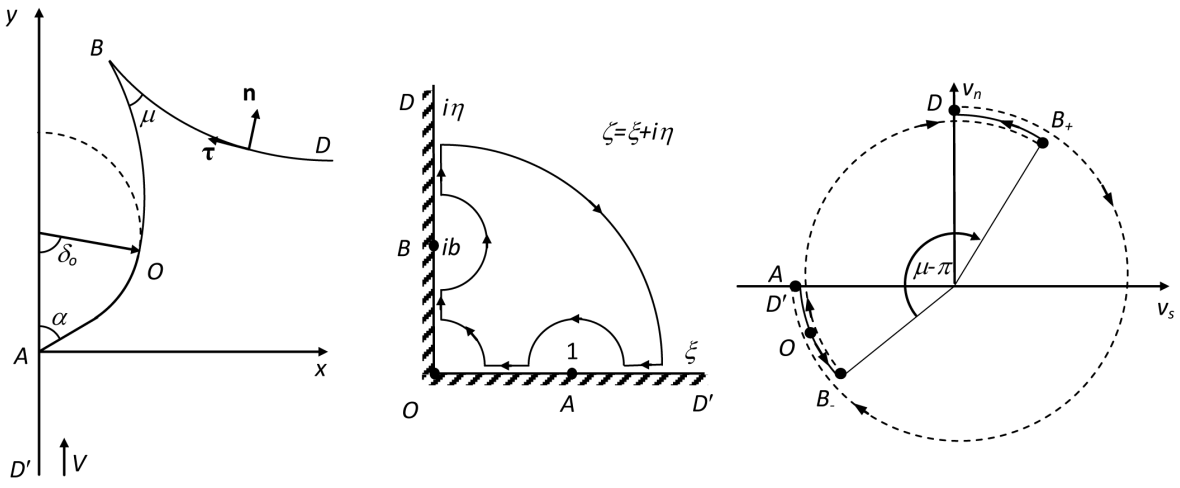


a b c

Fig. 1. Continuous and step changes are shown by solid lines and dashed lines, respectively (for a blunt body, the angle $\alpha = \pi/2$):
$a$ — similarity plane $z = x + iy$, of the vertical water-entry of an expanding shaped body;
$b$ — the $\zeta$ plane where arrows in the closed line show the path of integration in (11), which is opposite to the direction of vector $\tau$ and variable $S$;
$c$ — variation of the velocity angle $\omega(\zeta) = \arg(v_s + iv_n)$ to the flow boundary along the entire of the flow region

### 2.1. Expression for the complex velocity $dw/dz$

At this stage we assume that the velocity direction along the body, or the function $\beta(\xi) = -\arg(dw/dz)_{\zeta=\xi}$, and the velocity magnitude on the free surface $OBD$, or the function $v(\eta) = |dw/dz|_{\zeta=i\eta}$, are the known functions of the coordinates of the real and imaginary axes, respectively. With these notations, we have

$$\chi(\xi) = \arg\left(\frac{dw}{dz}\right) = \begin{cases} -\beta(\xi), & 0 < \xi < 1, \quad \eta = 0, \\ -\pi/2, & 1 < \xi < \infty, \quad \eta = 0. \end{cases} \tag{4}$$

$$\left|\frac{dw}{dz}\right| = v(\eta), \qquad 0 < \eta < \infty, \qquad \xi = 0. \tag{5}$$

The following integral formula (Semenov and Iafrati [14], Semenov and Cummings [20]) makes it possible to solve the mixed boundary value problem (4) and (5) respect to the complex function $dw/dz$:

$$\frac{dw}{dz} = v_\infty \exp\left[\frac{1}{\pi}\int_0^\infty \frac{d\chi}{d\xi} \ln\left(\frac{\zeta+\xi}{\zeta-\xi}\right) d\xi - \frac{i}{\pi}\int_0^\infty \frac{d\ln v}{d\eta} \ln\left(\frac{\zeta - i\eta}{\zeta + i\eta}\right) d\eta + i\chi_\infty\right], \tag{6}$$

where $v_\infty = 1$ due to the chosen velocity at infinity (point $D$, $\zeta \to \infty$) as the reference velocity, $V$, and $\chi_\infty = -\pi/2$ along the line of symmetry $AD'$. The velocity direction, or the function $\chi(\xi)$, has jump $\Delta\chi_A = \alpha$ at point $A$ ($\xi = 1$) since $\beta(\xi) \to \pi/2 - \alpha$ as $\xi \to 1 - \varepsilon$,

and $\beta(\xi) = \pi/2$ as $\xi \to 1+\varepsilon$, where $\varepsilon \to 0$. Using (4) and evaluating the integral over the jump of the function $\chi(\xi)$, equation (6) becomes

$$\frac{dw}{dz} = v_0 \left(\frac{\zeta-1}{\zeta+1}\right)^{\alpha/\pi} \times \\ \times \exp\left[\frac{1}{\pi}\int_0^1 \frac{d\beta}{d\xi} \ln\left(\frac{\xi-\zeta}{\xi+\zeta}\right) d\xi - \frac{i}{\pi}\int_0^\infty \frac{d\ln v}{d\eta} \ln\left(\frac{i\eta-\zeta}{i\eta+\zeta}\right) d\eta - i(\beta_0+\alpha)\right], \tag{7}$$

where $\beta_0 = \beta(\xi)_{\xi=0}$. The functions $\beta(\xi)$ and $v(\eta)$ will be determined later from the kinematic and dynamic boundary conditions.

### 2.2. Expression for the derivative of the complex potential $dw/d\zeta$

In order to obtain expression for the derivative of the complex potential it is useful to introduce the unit vectors $n$ and $\tau$ on the fluid boundary, which are normal and tangent to the flow boundary, respectively. The former is directed outward from the liquid region, and while one moves in the $\tau$ direction along the boundary, the arc length coordinate $s$ increases and the liquid region is on the left hand side (see Fig. 1a). With these notations, we have

$$dw = (v_s + iv_n)ds = ve^{i\omega}ds, \tag{8}$$

where $\omega(\zeta) = \arg(v_s + iv_n)$, $v_n$ and $v_s$ are the normal and tangential velocity components, respectively. Variation of the function $\omega(\zeta)$ along the entire boundary of the liquid region is shown in (Fig. 1c). The arrows in (Fig. 1b) show the direction of variation of $\omega(\zeta)$ only. $\omega(\zeta)_{\zeta=\xi} = -\pi$ on the interval $1 < \xi < \infty$, since $v_n = 0$ and $v_s < 0$, and $\omega(\zeta)_{\zeta=\xi} = \gamma(\xi)$ on the interval $0 < \xi < 1$ corresponding to the wetted part of the body. $\theta(\eta) = \omega(\zeta)_{\zeta=i\eta}$ changes continuously along $OB$ and $BD$, or on the intervals $(0, b)$ and $(b, \infty)$ on the $\eta - axis$. At point $B$ $\theta(\eta)$ has a jump $\Delta_B = -\pi + \mu$, where $\mu$ is the angle at point $B$. Based on the above considerations, we can write the function $\omega(\zeta)$ as follows:

$$\omega(\zeta) = \arg\left(\frac{dw}{ds}\right) = \begin{cases} -\pi, & 1 < \zeta < \infty, \quad \eta = 0, \\ \gamma(\xi), & 0 < \zeta < 1, \quad \eta = 0, \\ \lambda(\eta), & \xi = 0, \quad 0 < \eta < b, \\ \lambda(\eta) + \Delta_B, & \xi = 0, \quad b < \eta < \infty, \end{cases} \tag{9}$$

where $\lambda(\eta)$ is a continuous function (9) allows us to determine the argument of the derivative of the complex potential:

$$\vartheta(\varsigma) = \arg\left(\frac{dw}{d\varsigma}\right) = \arg\left(\frac{dw}{ds}\right) + \arg\left(\frac{ds}{d\varsigma}\right) = \omega(\zeta) + \nu, \\ \nu = \begin{cases} 0, & 0 < \xi < \infty, \quad \eta = 0, \\ \pi/2, & \xi = 0, \quad 0 < \eta < \infty. \end{cases} \tag{10}$$

The function $\lambda(\eta)$ increases from $\lambda_0 = \theta(\eta)_{\eta=0} = \gamma(\xi)_{\xi=0} = \gamma_0$ at point $O$ to $\lambda_\infty = \lambda(\eta)_{\eta\to\infty} = \theta(\eta)_{\eta\to\infty} + \pi - \mu = 3/2\pi - \mu$ at point $D$ (see Fig. 1c). Therefore, the angle $\mu$ is determined as $\mu = 3/2\pi - \lambda_\infty$.

The following integral formula (Semenov and Iafrati [14], Semenov and Cummings [20]) makes it possible to solve the uniform boundary value problem (9) and (10) respect to the complex function $dw/d\zeta$:

$$\frac{dw}{d\zeta} = K \exp\left[\frac{1}{\pi}\int\limits_{\infty}^{0} \frac{d\vartheta}{d\xi}\ln(\zeta^2 - \xi^2)d\xi + \frac{1}{\pi}\int\limits_{0}^{\infty} \frac{d\vartheta}{d\eta}\ln(\eta^2 + \zeta^2)d\eta + i\vartheta_\infty\right], \tag{11}$$

where $K$ is a real factor and $\vartheta_\infty = \vartheta(\zeta)_{|\zeta|\to\infty}$. By substituting (9) and (10) into (11) and evaluating the integrals over each step change of the function $\vartheta(\zeta)$, we obtain

$$\frac{dw}{d\zeta} = K\zeta(\zeta^2 + b^2)^{\frac{\mu}{\pi}-1} \exp\left[-\frac{1}{\pi}\int\limits_{0}^{\infty} \frac{d\gamma}{d\xi}\ln(\xi^2 - \zeta^2)d\xi + \frac{1}{\pi}\int\limits_{0}^{\infty} \frac{d\lambda}{d\eta}\ln(\eta^2 + \zeta^2)d\eta + i\gamma_0\right]. \tag{12}$$

The integration of this equation allows us to obtain the function of the complex potential, $w(\zeta)$:

$$\begin{aligned} w(\zeta) = w_A + K\int\limits_{1}^{\zeta} \zeta'(\zeta'^2 + b^2)^{\mu/\pi-1}\times \\ \times \exp\left[-\frac{1}{\pi}\int\limits_{0}^{\infty} \frac{d\gamma}{d\xi}\ln(\xi^2 - \zeta'^2)d\xi + \frac{1}{\pi}\int\limits_{0}^{\infty} \frac{d\lambda}{d\eta}\ln(\eta^2 + \zeta'^2)d\eta + i\gamma_0\right] d\zeta'. \end{aligned} \tag{13}$$

From (7) and (12) the derivative of the mapping function can be obtained as

$$\begin{aligned} \frac{dz}{d\zeta} = \frac{K}{v_0}\zeta(\zeta^2 + b^2)^{\mu/\pi-1}\left(\frac{\zeta+1}{\zeta-1}\right)^{\alpha/\pi}\times \\ \times \exp\left[-\frac{1}{\pi}\int\limits_{0}^{\infty} \frac{d\beta}{d\xi}\ln\left(\frac{\xi-\zeta}{\xi+\zeta}\right)d\xi + \frac{i}{\pi}\int\limits_{0}^{\infty} \frac{d\ln v}{d\eta}\ln\left(\frac{i\eta-\zeta}{i\eta+\zeta}\right)d\eta - \right. \\ \left. -\frac{1}{\pi}\int\limits_{0}^{\infty} \frac{d\gamma}{d\xi}\ln(\xi^2 - \zeta^2)d\xi + \frac{1}{\pi}\int\limits_{0}^{\infty} \frac{d\lambda}{d\eta}\ln(\eta^2 + \zeta^2)d\eta + i\gamma_0\right]. \end{aligned} \tag{14}$$

Integration of the above equation in the parameter region yields the mapping function $z = z(\zeta)$ relating the parameter and similarity planes.

In the physical plane the position of point $B$, $Z_B = Vtz_B$, can be related to the particle velocity at the tip of the splash jet, which is the constant $Vv_Be^{i\beta_B}$. Thus we can write

$$|z_B| = v_B, \tag{15}$$

where the left hand side $z_B = z(\zeta)_{\zeta=ib}$ and $v_B = v(\eta)_{\eta=b}$ from which the parameter $K$ is determined.

The parameter $b$ is the free parameter of the solution, which determines the expansion speed of the cylinder. For steady Helmholtz flow point $B$ approached point $D$, or $b \to \infty$ as can be seen from (Fig. 1 b). The velocity magnitude on the free surface is constant, $v(\eta) \equiv v_\infty$, or $d\ln v/d\eta \equiv 0$ and the normal component of the velocity on the free surface is zero, which means $\lambda(\eta) \equiv \theta(\eta) \equiv 0$ and $\gamma(\xi) \equiv 0$. Then, the angle at point $B$ becomes $\mu = 3\pi/2 - \lambda_\infty = \pi/2$. By substituting these expressions into (7) and (12) we obtain

$$\frac{dw}{dz} = v_0 \left(\frac{\zeta-1}{\zeta+1}\right)^{\frac{\alpha}{\pi}} \exp\left[\frac{1}{\pi}\int_0^1 \frac{d\beta}{d\xi} \ln\left(\frac{\xi-\zeta}{\xi+\zeta}\right) d\xi - i(\beta_0+\alpha)\right], \tag{16}$$

$$\frac{dw}{d\zeta} = K\zeta, \tag{17}$$

which is the solution for steady Helmholtz flow past the fixed curvilinear body.

Eqs. (7), (12)–(14) contain the functions $\beta(\xi)$, $\gamma(\xi)$, $v(\eta)$ and $\lambda(\eta)$, which have to be determined from the dynamic and kinematic boundary conditions on the free surface and the wetted part of the body.

### 2.3. Determination of the functions $v(\eta)$ and $\lambda(\eta)$ on the free surface

By exploiting the Bernoulli equation and taking the advantage of the flow self-similarity, the dynamic boundary conditions on the free surface $OBD$ can be derived in the following form (Semenov and Iafrati [14]),

$$\frac{d\lambda}{d\eta} = \frac{v + s\cos\theta}{s\sin\theta}\frac{d\ln v}{d\eta}, \tag{18}$$

where $d\lambda/d\eta = d\theta/d\eta$ from (9) is used. The arc length coordinate along the free surface with its origin at point $B$ is determined as

$$s(\eta) = -\int_b^\eta \left|\frac{dz}{d\zeta}\right|_{\zeta=i\eta'} d\eta' = -\int_b^\eta \frac{|dw/d\zeta|_{\zeta=i\eta'}}{|dw/dz|_{\zeta=i\eta'}} d\eta' = -\int_b^\eta \frac{1}{v(\eta')}\left|\frac{dw}{d\zeta}\right|_{\zeta=i\eta'} d\eta', \tag{19}$$

where $dw/d\zeta$ is used from (12).

The kinematic boundary is obtained in the following form by exploiting the fact that the acceleration of a liquid particle is orthogonal to the free surface along which the pressure is constant:

$$\frac{1}{\operatorname{tg}\theta}\frac{d\ln v}{d\eta} = \frac{d}{d\eta}\left[\arg\left(\frac{dw}{dz}\right)\right]. \tag{20}$$

Determining the argument of the complex velocity from (7) and substituting the result into (20) the following integral equation for the function $d\ln v/d\eta$ is obtained:

$$-\frac{1}{\operatorname{tg}\theta}\frac{d\ln v}{d\eta} + \frac{1}{\pi}\int_0^\infty \frac{d\ln v}{d\eta'}\frac{2\eta'}{\eta'^2-\eta^2}d\eta' = \frac{2\alpha}{\pi}\frac{1}{1+\eta^2} + \frac{1}{\pi}\int_0^\infty \frac{d\beta}{d\xi}\frac{2\xi}{\xi^2+\eta^2}d\eta'. \tag{21}$$

The system of equations (15) and (17) enables us to determine the functions $\theta(\eta)$ and $d\ln v/d\eta$ along the imaginary axis of the parameter plane. Then, the velocity magnitude on the free surface and the function $\lambda(\eta)$ can be obtained from

$$v(\eta) = \exp\left(-\int_{\eta}^{\infty} \frac{d\ln v}{d\eta'} d\eta'\right), \tag{22}$$

$$\lambda(\eta) = \gamma_0 + \int_{0}^{\eta} \frac{d\lambda}{d\eta'} d\eta'. \tag{23}$$

This gives the velocity $v_0 = v(\eta)_{\eta=0}$ and the contact angle $\mu = 2\pi/3 - \lambda_\infty$, where $\lambda_\infty = \lambda(\eta)_{\eta\to\infty}$.

### 2.4. Determination of functions $\beta(\xi)$ and $\gamma(\xi)$ on the body surface

The normal component of the velocity on the expanding body can be determined exploiting the fact that the body surface $Z_b = Z_b(S)$ is a given self-similar surface. By using the self-similar variable $z = Z/(Vt)$ we can write $Z_b = Vtz_b(s)$, and the slope of the body $\delta_b(S) = \delta_b(s) = \arg(dz_b/ds)$. With notation in (8) and using $ds/dt|_S = -s/t$, we obtain

$$dW = V^2 t dw = V^2 t(v_s + iv_n)ds = \frac{\overline{dZ_b}}{dt} dZ = Vt\frac{\overline{dZ_b}}{dt}\frac{dz_b}{ds} ds = V^2 t(\bar{z}_b - e^{-i\delta_b} s)e^{i\delta_b} ds,$$

from which the normal component of the velocity on the body is obtained as

$$v_n(s) = \mathbf{Im}\,(\bar{z}_b e^{i\delta_b(s)}). \tag{24}$$

The tangential component of the velocity on the body can be determined with the notation in (8):

$$v_s(\xi) = \mathbf{Re}\left(\frac{dw}{dz}\frac{dz}{ds}\right) = \mathbf{Re}\left(\frac{dw}{dz}\Big|_{\zeta=\xi} e^{i\delta_b[s(\xi)]}\right), \tag{25}$$

where

$$s(\xi) = \int_{1}^{\xi} \frac{ds}{d\xi'} d\xi' = \int_{1}^{\xi} \left|\frac{dz}{d\zeta}\right|_{\zeta=\xi'} d\xi' \tag{26}$$

is the arc length coordinate along the body with its origin at point $A$, and $dz/d\zeta$ from (14) is used.

By using (24), (25) and the definition of the function $\gamma(\xi)]$ we can obtain

$$\gamma(\xi) = \mathrm{tg}^{-1}\left\{\frac{\mathbf{Im}\,(\bar{z}_b[s(\xi)]e^{i\delta_b[s(\xi)]})}{\mathbf{Re}\,(dw/dz|_{\zeta=\xi} e^{i\delta_b[s(\xi)]})}\right\}. \tag{27}$$

The angle $\delta_b$ between the unit vector $\tau$ and $x$-axis is determined by the given shape of the body which can be expressed through the angles $\beta$ and $\gamma$. Taking the argument of (14) and recall that $\beta(\xi) = -\arg(dw/dz)_{\zeta=\xi}$ and $\lambda(\xi) = \omega(\zeta)_{\zeta=\xi} = \arg(dw/ds)$ we obtain $\delta_b = \beta + \gamma$, from which the function $\beta(\xi)$ is obtained as

$$\beta(\xi) = \delta_b[s(\xi)] - \gamma(\xi). \tag{28}$$

The equations (27) and (28) allows us to determine the functions $\gamma(\xi)$ and $\beta(\xi)$.

### 2.5. The condition of flow detachment

According to the Brillouin–Villat criterion of flow detachment from shaped bodies, the curvature of the free streamline should be equal to the curvature of the body at the point of detachment. This criterion has been derived for steady flows (Brillouin [24], Villat [25]). We show that this criterion is also valid to the determination of flow detachment for unsteady flows.

We introduce the function $\delta(\eta) = \bar{\beta}(\eta) + \theta(\eta)$, which is the slope of the free surface. Here, $\bar{\beta}(\eta)$ is the velocity direction on the free surface, which is obtained from (7) at $\zeta = i\eta$ as

$$\begin{aligned}\bar{\beta}(\eta) = -\mathbf{Im}\left(\ln\frac{dw}{dz}|_{\zeta=i\eta}\right) = \\ = \frac{2\alpha}{\pi}\arctan\eta + \frac{2}{\pi}\int\limits_0^1 \frac{d\beta}{d\xi}\arctan\frac{\eta}{\xi}d\xi + \frac{1}{\pi}\int\limits_0^1 \frac{d\ln v}{d\eta'}\ln\left|\frac{\eta'-\eta}{\eta'+\eta}\right|d\eta' + \beta_0.\end{aligned} \tag{29}$$

On the free surface in (8) $\omega(\zeta)_{\zeta=i\eta} = \theta(\eta)$, therefore we can write $dw/ds = ve^{i\theta}$. On the other hand, $dw/ds = (dw/dz)(dz/ds) = e^{i\delta}dw/dz$. Thus, we have the following relation:

$$ve^{i\theta} = \frac{dw}{dz}e^{i\delta}. \tag{30}$$

By differentiating the left- and right-hand sides of the above equation with respect to $s$ we obtain

$$ve^{i\theta}\left(\frac{d\ln v}{ds} + i\frac{d\theta}{ds}\right) = e^{2i\delta}\frac{d^2w}{dz^2} + ie^{i\delta}\frac{dw}{dz}\frac{d\delta}{ds}. \tag{31}$$

The term $d^2w/dz^2$ on the right-hand side of the above equation is a bounded function because the complex velocity given by (7) is the analytical function, which is finite at the point of flow detachment. From the above equation it follows that the function $|d\theta/ds| < \infty$ if the curvature of the free surface is also bounded, $|d\delta/ds| < \infty$.

The curvature of the free surface can be determined as $\kappa = d\delta/ds$ which at the detachment point $O$ is

$$\kappa_O = \lim_{s\to 0}\left(\frac{d\bar{\beta}}{ds} + \frac{d\theta}{ds}\right) = \lim_{\eta\to 0}\frac{\frac{d\bar{\beta}}{d\eta}}{\frac{ds}{d\eta}} + \lim_{s\to 0}\frac{d\theta}{ds}. \tag{32}$$

Differentiating (29) and taking into account that the leading order of $ds/d\eta$ at point $O$ ($\eta = 0$) is

$$\frac{ds}{d\eta} \sim -\frac{K_1\eta}{v(\eta)}, \tag{33}$$

where

$$K_1 = Kb^{\frac{2\mu}{\pi}-2}\exp\left[-\frac{2}{\pi}\int\limits_0^\infty \frac{d\gamma}{d\xi}\ln\xi d\xi + \frac{2}{\pi}\int\limits_0^\infty \frac{d\lambda}{d\eta'}\ln\eta' d\eta'\right],$$

we obtain

$$\kappa_O = \lim_{\eta\to 0}\left[-\frac{v(\eta)}{K_1\eta}\left(\frac{2\alpha}{\pi}\frac{1}{1+\eta^2} + \frac{2}{\pi}\int\limits_0^1 \frac{d\beta}{d\xi}\frac{\xi d\xi}{\xi^2+\eta^2} - \frac{2}{\pi}\int\limits_0^1 \frac{d\ln v}{d\eta'}\frac{\eta' d\xi}{\eta'^2-\eta^2}\right)\right] + \left.\frac{d\theta}{ds}\right|_{s=0}. \tag{34}$$

From (34) it follows, that the curvature of the free surface takes a finite value if the expression in the parenthesis tends to zero as $\eta \to 0$. In other case, the curvature becomes infinite that leads to the intersection of the body and the free surface. Thus, the following condition is obtained,

$$\frac{1}{\pi}\int\limits_0^1 \frac{d\beta}{d\xi}\frac{d\xi}{\xi} - \frac{1}{\pi}\int\limits_0^1 \frac{d\ln v}{d\eta'}\frac{d\eta'}{\eta'} + \frac{\alpha}{\pi} = 0, \tag{35}$$

from which the position of the point of flow detachment, which affects the function $d\beta/d\xi = (d\beta/ds) \times (ds/d\xi)$ is determined.

In order to evaluate the curvature of the free surface at point $O$ ($\eta \to 0$), we differentiate the numerator and denominator of (34) to resolve its indeterminate, then obtain

$$\begin{aligned}\kappa_O = \left.\frac{d\theta}{ds}\right|_{s=0} + \\ + \lim_{\eta\to 0}\left[-\frac{1}{K_1}\frac{d\ln v}{d\eta}\left(\frac{2\alpha}{\pi}\frac{1}{1+\eta^2} + \frac{2}{\pi}\int\limits_0^1 \frac{d\beta}{d\xi}\frac{\xi d\xi}{\xi^2+\eta^2} - \frac{2}{\pi}\int\limits_0^1 \frac{d\ln v}{d\eta'}\frac{\eta' d\xi}{\eta'^2-\eta^2}\right) + \right. \\ \left. + \frac{2v\eta}{K_1}\left(\frac{2\alpha}{\pi}\frac{1}{(1+\eta^2)^2} + \frac{2}{\pi}\int\limits_0^1 \frac{d\beta}{d\xi}\frac{\xi d\xi}{(\xi^2+\eta^2)^2} - \frac{2}{\pi}\int\limits_0^1 \frac{d\ln v}{d\eta'}\frac{\eta' d\xi}{(\eta'^2-\eta^2)^2}\right)\right].\end{aligned} \tag{36}$$

The first term in the above equation equals zero due to (35). In order to evaluate the second term containing the singular integrals, we have to estimate the leading order of the functions $d\ln v/d\eta$ at $\eta \to 0$ and $d\beta/d\xi$ at $\xi \to 0$:

$$\left.\frac{d\ln v}{d\eta}\right|_{\eta\to 0} = \left.\frac{d\ln v}{ds}\right|_{s\to 0}\left.\frac{ds}{d\eta}\right|_{\eta\to 0} \sim \eta^{1+\varepsilon}, \qquad \varepsilon \geq 0. \tag{37}$$

$$\left.\frac{d\beta}{d\xi}\right|_{\xi\to 0} = \left.\frac{d\beta}{ds}\right|_{s\to 0}\left.\frac{ds}{d\xi}\right|_{\xi\to 0} = \left(\left.\frac{d\delta_b}{ds}\right|_{s\to 0} - \left.\frac{d\gamma}{ds}\right|_{s\to 0}\right)\left.\frac{ds}{d\xi}\right|_{\xi\to 0} \sim \left(\kappa_b - \left.\frac{d\gamma}{ds}\right|_{s\to 0}\right)\frac{K_1}{v_0}\xi, \tag{38}$$

where $\kappa_b = -(d\delta_b/ds)_{s=0}$ is the curvature of the body at the point of flow detachment.

By substituting the estimates (37) and (38) of the functions $d\ln v/d\eta$ and $d\beta/d\xi$ into the corresponding integrals in (36) and taking into account that

$$\lim_{\eta\to 0}\eta\int\limits_0^\infty \frac{\eta'^{2+\varepsilon}d\eta'}{(\eta'^2-\eta^2)^2} = 0, \qquad \lim_{\eta\to 0}\eta\int\limits_0^\infty \frac{\xi'^2 d\xi'}{(\xi'^2+\eta^2)^2} = \frac{\pi}{4} \tag{39}$$

we can find that the curvature of the free surface at the point of flow separation is equal to the curvature of the body, i.e.,

$$\kappa_O = \kappa_b - \left.\frac{d\gamma}{ds}\right|_{s=0} + \left.\frac{d\theta}{ds}\right|_{s=0} = \kappa_b, \tag{40}$$

where $(d\gamma/ds)_{s=0} = (d\theta/ds)_{s=0}$ that follows from the definition of functions $\gamma(\xi) = \omega(\zeta)_{\zeta=\xi}$ and $\theta(\eta) = \omega(\zeta)_{\zeta=i\eta}$.

The system of integral equations (18), (21), (27), (28) lets us to determine the unknown functions $\theta(\eta)$, $v(\eta)$, $\gamma(\xi)$ and $\beta(\xi)$, and (35) determines the position of flow detachment. Once these functions are found, the free surface and the velocity field can be determined through the government expressions (7), (12)–(14).

The pressure coefficient $c_p$ based on the ambient pressure, $P_a$, and normalized by $\rho V^2/2$ where $\rho$ is the liquid density, can be evaluated in the same way as for the self-similar problem of impact between two liquid wedges (Semenov, Wu, Oliver [15]). By choosing the location of the reference point in Bernoulli equation at the stagnation point $A$ and taking the advantage of self-similarity, we can determine the pressure coefficient at any point of the flow region using

$$c_p^* = \frac{2(P-P_A)}{\rho V^2} = \mathbf{Re}\left(-2w + 2z\frac{dw}{dz}\right) - \left|\frac{dw}{dz}\right|^2. \tag{41}$$

Then, the pressure coefficient based on the ambient pressure, $P_a$, is determined as follows:

$$c_p(\xi) = \frac{2(P-P_a)}{\rho V^2} = c_p^*(\xi) - c_p^*(\xi)_{\xi=0}. \tag{42}$$

## 3. RESULTS AND DISCUSSION

The formulation of the problem and its solution derived in section 2 makes it possible to consider arbitrary shaped bodies including a wedge of the half-angle $\alpha$, that has been studied by Semenov and Wu [26]. In this section we have presented results for a circular cylindrical of radius $R$, which expands in time at constant speed $V_R$ during its entry into the liquid of infinite depth at constant vertical velocity $V$. The general solution contains the free parameter $b$ which determines the relative expansion speed $u = V_R/V$.

The solution procedure of the system of integral equations is similar to that in Semenov and Wu [26], and it is based on the method of successive approximations. In discrete form, the solution is sought on a fixed set of points $\xi_j$, $j = 1, \ldots, M$ distributed along the real axis of the parameter region and on a fixed set of points $\eta_j$, $j = 1, \ldots, N$ distributed along the imaginary axis. The intervals $(\eta_1, \eta_{N_b})$ and $(\eta_{N_b}, \eta_N)$ correspond to the segments $OB$ and $BD$, respectively. The nodes $\eta_j$ are distributed as a geometric series with higher density near the singular point $\eta_{N_b} = b$ corresponding to the tip of the splash jet. The integrand of (19) determining the arc length coordinate has singularity $|\eta - b|^{\mu/\pi - 1}$ that requires to evaluate the nodes $s_{N_b-1}$ and $s_{N_b+1}$ nearest to point $B$ analytically. Using (19) we obtain

$$s_{\{N-1,N+1\}} = \mp\frac{\pi K b^{\mu/\pi}}{\mu v_B 2^{1-\mu/\pi}} \times \\ \times \exp\left[-\frac{1}{\pi}\int_0^\infty \frac{d\gamma}{d\xi}\ln(\xi^2+b^2)d\xi + \frac{1}{\pi}\int_0^\infty \frac{d\lambda}{d\eta'}\ln|\eta'^2 - b^2|d\eta'\right]|\eta_{\{N-1,N+1\}} - b|^{\mu/\pi}, \tag{43}$$

where $v_B = v(\eta)_{\eta=b}$. It is seen that the smaller contact angle $\mu$, the larger arc lengths of the nodes $s_{N_b-1}$ and $s_{N_b+1}$ nearest to the tip of the splash jet (point $B$).

The angle of the splash jet is an important parameter because it influences the spatial arc length coordinate starting at the tip of the jet. If we are able to obtain a good accuracy

Tab. 1. Tip angle of the splash jet and the length of the node $s_{N_b-1}$ nearest to the tip of the jet in the similarity plane referred to the length of the splash jet at $b = 10^{-5}$. The columns correspond to different intervals between the singular point $\eta_{N_b} = b$ and the nearest node $\eta_{N_b-1}$. The rows correspond to different numbers of nodes

| | $\mu/\pi$ | | | $s_{N_b-1}/s_{OB}$ | | |
|---|---|---|---|---|---|---|
| $b - \eta_{N_b-1}$ | $N = 100$ | $N = 200$ | $N = 400$ | $N = 100$ | $N = 200$ | $N = 400$ |
| $10^{-6}$ | 0.000606 | 0.000567 | 0.000547 | 0.99764 | 0.99830 | 0.99833 |
| $10^{-7}$ | 0.000611 | 0.000569 | 0.000551 | 0.99518 | 0.99596 | 0.99604 |
| $10^{-8}$ | 0.000617 | 0.000572 | 0.000553 | 0.99230 | 0.99354 | 0.99361 |

for the jet angle, then we can be sure that the accuracy for the other parameters is good too. Tab. 1 gives the splash jet angle $\mu$ and the of the arc lengths of the nodes $s_{N_b-1}$ and $s_{N_b+1}$ referred to the length of the splash jet between points $O$ and $B$, $s_{OB}$, predicted for $b = 10^{-5}$. It is seen that the arc length of the node $s_{N_b-1}$ is about 99

The solution converges when both the number $N \to \infty$ and the smallest interval $\Delta \to 0$. At a fixed $\Delta$ the accuracy is increased with increasing $N$. The node distribution geometry is such that for too small values of $\Delta$ the node density becomes higher near the singular points and lower for the rest of the corresponding interval, which may decrease the overall integration accuracy. The values $\Delta = 10^{-6}$, $N = 400$ and $M = 200$ have been found sufficiently to provide reasonable accuracy of results.

In Fig. 2 are shown the streamline patterns at different values of $b$, or the expansion speed $u$. The wetted surface of the cylinder is shown by the thick line and non wetted surface is shown by the dashed line. The slopes of the streamlines show the instant flow velocity direction, and their density shows the velocity magnitude, since the flowrate between the streamlines is constant. The higher density of the streamlines occurs near the core of the splash jet. The tip angle of the splash jet is so small that lines corresponding to the sides of the jet are overlaps. The zero streamline starting at the origin divides the inflow liquid coming from infinity and the liquid displayed by the cylinder due to its expansion. In Fig. 2 it is also seen that the larger expansion speed, the larger length of the splash jet, while its inclination to the $x$-axis becomes smaller. At the large expansion speeds, the length of the splash jet becomes comparable with the length of the wetted part of the cylinder.

For the flow patterns shown in (Fig. 2b–e) the expansion speed gradually decreases. The angle of flow detachment from the cylinder, $\delta_o$, measured from the bottom point increases for the expansion speeds in the range $0.8 < u < \infty$, and then it starts to decrease for further decrease of the expansion speed in the rang $0 < u < 0.8$. For the very small expansion speed shown in (Fig. 2f) the angle $\delta_o$ approaches the value $\delta_o = 55°$ which is the angle of flow detachment for the steady flow past a circular cylinder (Gurevich [23]). In this case, the length of the free surface $OB$ increases forming the cavity. The flow approaches the steady free streamline flow past the cylinder of the fixed size. It is known that the half width of the steady cavity, $X_c$, tends to infinity at a rate of $X_c \sim \ln Y_c \sim \ln Vt$. However, in the similarity plane the coordinate $x_c = X_c/(Vt) \sim \ln Vt/(Vt) \to 0$ as it seen in (Fig. 2f).

The drag force coefficient $C_D$ is obtained by integration of the pressure along the wetted

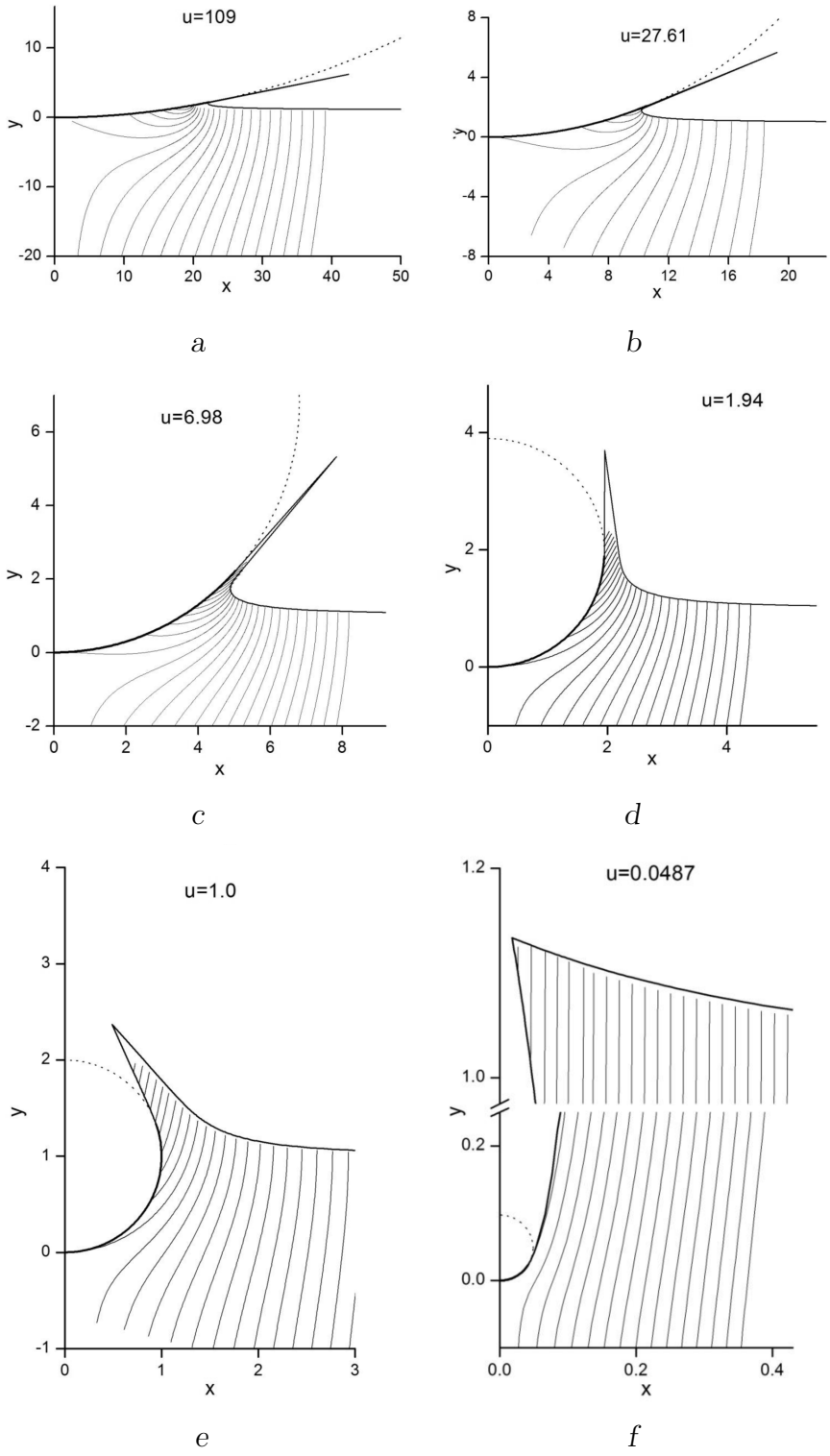


Fig. 2. The free surface shape and streamlines for different expansion speeds of a circular cylinder: a — $u = 195$, $b = 10^{-6}$; $b$ — $u = 18.6$, $b = 10^{-4}$; $c$ — $u = 10.01$, $b = 5 \cdot 10^{-4}$; $d$ — $u = 1.94$, $b = 10^{-2}$; $e$ — $u = 0.837$, $b = 0.1$; $f$ — $u = 0.0487$

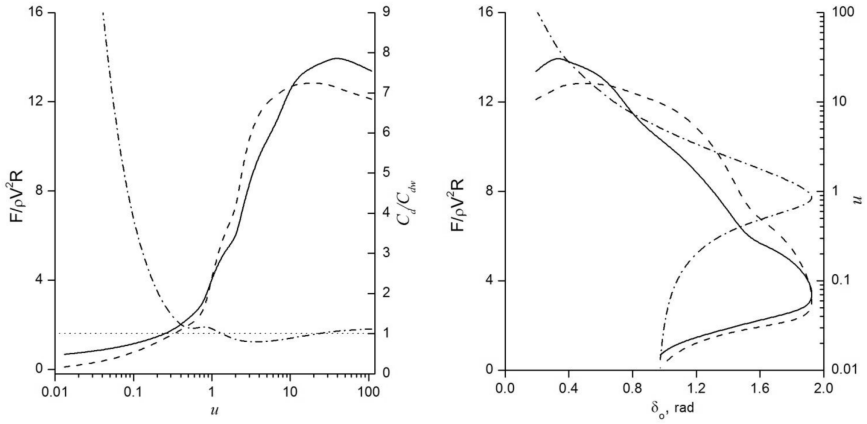


a b

Fig. 3. Impact force on an expanding circular cylinder entering water with constant velocity: *a* — as a function of expansion velocity $u$, *b* — as a function of detachment angle $\delta_0$; *solid lines* — present predictions, *dashed line* — model of expansion flat plate, *dash-dotted line in a* — ratio of the force coefficients corresponding to the expanding circle and flat plat, *dash-dotted line in b* — expansion velocity

part of the cylinder:

$$C_d = \frac{2}{\rho V^2 R}\int\limits_{S_O}^{S_A}[P(S) - P_a]\cos\delta_b(S)dS = \frac{1}{u}\int\limits_0^1 c_p[s(\xi)]\cos\delta_b[s(\xi)]\frac{ds}{d\xi}d\xi, \tag{44}$$

where $R = Vut$ is the radius of the cylinder.

For comparison purposes we compute the drag force based on the Wagner's slamming model, which is based on the flat plate approximation of the shaped body. In this model the flat plate links the core points of the splash jets on the left and right hand sides of the body. The force predicted by Wagner model for the case of the constant entry speed can be expressed analytically (Faltinsen [17]):

$$F = \rho\pi V L\frac{dL}{dt} = \rho V^2 R C_{dp}, \tag{45}$$

where $L$ the half length of the flat plate, and $C_{dp}$ is the force coefficient. This equation is obtained assuming that the local fluid accelerations much higher that convective term in the Euler equation, or the term $v^2/2$ in Bernoulli equation can be neglected. In the case of the expanding circular cylinder, the half length of the equivalent flat plate is $L = R\sin\delta_0 = Vtu\sin\delta_0$ (see Fig. 1a), and the angle of flow detachment $\delta_0$ is constant. We note that the core point of the splash jet and the point of flow detachment are very close each other, as it is seen in Fig. 2 at the large expansion speeds. By substituting $L$ into above equation, we obtain the coefficient of the drag force coefficient as

$$C_{dp} = \pi u\sin^2\delta_o(u). \tag{46}$$

In Fig. 3 are shown the force predicted by the expanding circular cylinder and the expanding flat plate models. It is seen in (Fig. 3a), that agreement between these models is

quite good. The dash-dotted line in (Fig. 3a) shows the ratio of these force coefficients. This ratio changes between 0.8 and 1.1 in the range of the expansion velocities $0.5 < u < 100$. For smaller expansion speeds, the force predicted the circular cylinder model becomes larger than that based on the flat plate model. It is due to the fact that $C_{dp} \to 0$ as $u \to 0$ according to (45), while the self-similar solution predicts the force corresponding to the steady flow past the circular cylinder. The force coefficient as function of the angle of flow detachment is shown in (Fig. 3b). A good agreement could be expected for large expansion velocities, or for the cases corresponding to (Fig. 2a) and (Fig. 2b), for which the local deadrise angles are relatively small. However, the same good agreement occurs for larger local deadrise angles up to $\delta_0 = 1.9$ rad, or 110°. These results show that the model based on the flat plate approximation of a shaped body can predict the force quite well if the point of intersection of the free surface and the body has been determined precisely.

The expansion velocity $u$, the angle of flow detachment, $\delta_0$, the tip angle of the splash jet, $\mu$, and the drag coefficients, $C_d$ and $C_{dp}$, for various values of the parameter $b$ are shown in Tab. 2. We note, that force coefficients $C_d$ and $C_{dp}$ about twice larger than that for a cylinder of the fixed radius, $R^*$, at small deadrise angles predicted by the Wagner's model (Oliver [27]). This difference shows the effect of flow history before time $t = R^*/Vu$ at which the radius of the expanding cylinder $R = Vtu = R^*$.

The results in Tab. 2 show that for $b \to 0$ the angle of the splash jet, $\mu$, tends to zero, and

Tab. 2. Main reference parameters for water-entry of an expanding circular cylinder with detached splash jet. In the last line are shown the values corresponding to the steady flow past a circular cylinder (Gurevich [23])

| $u$ | $b$ | $\delta_0$ | $\mu/\pi$ | $C_d$ | $C_{dp}$ |
|---|---|---|---|---|---|
| 108.78142 | 0.00001 | 0.193121 | 0.000550 | 14.0868 | 12.11771 |
| 41.55721 | 0.00005 | 0.31924 | 0.001414 | 13.7964 | 12.58802 |
| 27.65391 | 0.0001 | 0.39457 | 0.002131 | 13.2002 | 12.85957 |
| 10.99848 | 0.0005 | 0.64111 | 0.005596 | 11.1197 | 12.83803 |
| 7.01799 | 0.001 | 0.81758 | 0.009264 | 9.796 | 12.35972 |
| 4.10257 | 0.0025 | 1.08471 | 0.017411 | 7.9778 | 11.73287 |
| 2.78384 | 0.005 | 1.31627 | 0.027933 | 6.5717 | 10.0757 |
| 2.24591 | 0.0075 | 1.45413 | 0.036389 | 5.7907 | 8.191236 |
| 1.9481 | 0.01 | 1.54699 | 0.04310 | 5.2751 | 6.960128 |
| 1.42923 | 0.02 | 1.74132 | 0.063460 | 4.2287 | 6.116664 |
| 1.0313 | 0.05 | 1.90483 | 0.09384 | 3.2406 | 4.360752 |
| 0.8387 | 0.1 | 1.94022 | 0.12134 | 2.7027 | 2.89372 |
| 0.6899 | 0.2 | 1.87870 | 0.15255 | 2.2778 | 2.291327 |
| 0.5012 | 0.5 | 1.61454 | 0.20051 | 1.7345 | 1.968317 |
| 0.3230 | 1 | 1.32409 | 0.24315 | 1.2694 | 1.571554 |
| 0.1464 | 2 | 1.10389 | 0.28943 | 0.8814 | 0.954216 |
| 0.0477 | 4 | 1.00520 | 0.33597 | 0.6708 | 0.366741 |
| 0.0131 | 8 | 0.97289 | 0.37923 | 0.5761 | 0.106814 |
| 0 | $\infty$ | 0.959931 | – | 0.4986 | |

the length of the splash jet increases. However, the flow configuration for $b \to 0$ is different from that for the case $b = 0$, for which points $B$ and $O$ coincides, and the singularity at point $B$ merges with zero at point $O$ that results in singularity of order $2\mu/\pi - 1$ at point $O$.

## 4. CONCLUSIONS

Analytical self-similar solutions for water entry of an expanding shaped body with flow detachment have been presented. The integral hodograph method has been employed to derive the complex potential of the flow defined in the parameter plane and the mapping function providing the relation between the similarity and parameter planes. Through the method, the problem is reduced to a system of integral and integro-differential equations after the dynamic and kinematic boundary conditions on the free surface and the body are imposed. The Brillouin–Villat condition of flow detachment has been reconsidered for the case of unsteady flows. It was shown that it keeps the same form as it is for steady flows. The curvature of the free surface at the point of flow detachment has been derived and shown that the Brillouin–Villat criterion of flow detachment is satisfied for unsteady flows too.

The solution of the problem includes a free parameter $b$ whose choice determines the expansion speed of the body and covers two limiting cases. For $b \to \infty$, the expansion speed $u = 0$, thus the steady free-streamline Helmholtz flow past the shaped body with infinite cavity is obtained as the special case. For $b = 0$ the solution describes the flow with the splash jet attached to the body. The analysis of the obtained results and their comparisons with that based on the simplified expanding flat plate model revealed that the difference of the predicted force is less than 20% in the wide range of local deadrise angles from 0 to 110 degrees. At the same time the drag force predicted by the model of the expanding circular cylinder is about twice larger than that corresponding to water impact of a circular cylinder of the fixed size. This may occurs due to the different elevation of the free surfaces corresponding to water entry of the expanding cylinder and that of a fixed size.

## REFERENCES

[1] The impact of seaplane floats during landing : Rep. / National Advisory Committee for Aeronautics ; executor: Karman T. — Washington : 1932. — P. 321.

[2] Wagner H. Über Stoß- und Gleitvorgänge an der Oberfläche von Flüssigkeiten // Zeitschrift für Angewandte Mathematik und Mechanik. — 1932. — Vol. 12. — P. 193–215.

[3] Mackie A. A linearized theory of the water entry problem // Quarterly Journal of Mechanics and Applied Mathematics. — 1962. — Vol. 15. — P. 137–151.

[4] Garabedian P. R. Oblique water entry of a wedge // Communications on Pure and Applied Mathematics. — 1953. — Vol. 6, no. 2. — P. 157–165.

[5] Garabedian P. R. Asymptotic description of a free boundary at the point of separation // Applications of nonlinear partial differential equations in mathematical physics / ed.

by Finn R. — Providence, RI : AMS. — 1965. — Vol. XVII of Proceedings of Symposia in Applied Mathematics. — P. 111.

[6] Cointe R., Armand J. L. Hydrodynamic impact analysis of a cylinder // Journal of Offshore Mechanics and Arctic Engineering. — 1987. — Vol. 109. — P. 237–243.

[7] Howison S. D., Ockendon J. R., Oliver J. M. Oblique slamming, planing and skimming // Journal of Engineering Mathematics. — 2004. — Vol. 48. — P. 321–337.

[8] Korobkin A. A. Analytical models of water impact // European Journal of Applied Mathematics. — 2004. — Vol. 15. — P. 821–838.

[9] Greenhow M. Wedge entry into initially calm water // Applied Ocean Research. — 1987. — Vol. 9. — P. 214–223.

[10] Mei X., Lui Y., Yue D. K. P. On the water impact of general two-dimensional sections // Applied Ocean Research. — 1999. — Vol. 21. — P. 1–15.

[11] Cumberbatch E. The impact of a water wedge on the wall // Journal of Fluid Mechanics. — 1960. — Vol. 7. — P. 353–374.

[12] Dobrovol'skaya Z. N. Some problems of similarity flow of fluid with a free surface // Journal of Fluid Mechanics. — 1969. — Vol. 36. — P. 805–829.

[13] Zhao R., Faltinsen O. Water-entry of two-dimensional bodies // Journal of Fluid Mechanics. — 1993. — Vol. 246. — P. 593–612.

[14] Semenov Y. A., Iafrati A. On the nonlinear water entry problem of asymmetric wedges // Journal of Fluid Mechanics. — 2006. — Vol. 547. — P. 231–256.

[15] Semenov Y. A., Wu G. X., Oliver J. M. Splash jet caused by collision of two liquid wedges // Journal of Fluid Mechanics. — 2013. — Vol. 737. — P. 132–145.

[16] Iafrati A., Korobkin A. A. Initial stage of flat plate impact onto liquid free surface // Physics of Fluids. — 2004. — Vol. 16. — P. 2214–2227.

[17] Faltinsen O. M. Hydrodynamics of high-speed marine vehicles. — Cambridge University Press, 2005. — P. 454.

[18] Shakeri M., Tavakolinejad M., Duncan J. H. An experimental investigation of divergent bow waves simulated by a two-dimensional plus temporal wave marker technique // Journal of Fluid Mechanics. — 2009. — Vol. 634. — P. 217–243.

[19] Aircraft ditching numerical simulation / Climent H., Benitez L., Rueda F., and Toso-Pentecote N. // ICAS 2006. — 2006.

[20] Semenov Y. A., Cummings L. J. Free boundary Darcy flows with surface tension: Analytical and numerical study // European Journal of Applied Mathematics. — 2006. — Vol. 17. — P. 607–631.

[21] Жуковский Н. Е. Видоизменение метода Кирхгофа для определения движения жидкости в двух измерениях при постоянной скорости, данной на неизвестной линии тока. — Москва : Московское математическое общество, 1890. — Т. XV из Математический сборник. — 159 с. — Режим доступа: http://books.e-heritage.ru/book/10070428.

[22] Michell J. H. On the theory of free stream lines // Philosophical Transactions of the Royal Society A. — 1890. — Vol. 181. — P. 389–431.

[23] Gurevich M. I. Theory of jets in ideal fluids. — New York : Academic Press, 1965. — P. 585.

[24] Brillouin M. Les surfaces de glissement de Helmholtz et la résistance des fluids // Annales de Chimie et de Physique. — 1911. — Vol. 23. — P. 145–230.

[25] Villat H. Sur la validité des solutions de certains problèmes d'Hydrodynamique // Journal de Mathématiques Pures et Appliquées. — 1914. — Vol. 10. — P. 231–290.

[26] Semenov Y. A., Wu G. X. Water entry of an expanding wedge/plate with flow detachment // Journal of Fluid Mechanics. — 2016. — Vol. 797. — P. 322–344.

[27] Oliver J. M. Second-order Wagner theory for two-dimensional water-entry problems at small deadrise angles // Journal of Fluid Mechanics. — 2007. — Vol. 572. — P. 59–85.

## REFERENCES

[1] T. Karman, "The impact of seaplane floats during landing," tech. rep., National Advisory Committee for Aeronautics, Washington, 1932.

[2] H. Wagner, "Über Stoß- und Gleitvorgänge an der Oberfläche von Flüssigkeiten," *Zeitschrift für Angewandte Mathematik und Mechanik*, vol. 12, pp. 193–215, 1932.

[3] A. Mackie, "A linearized theory of the water entry problem," *Quarterly Journal of Mechanics and Applied Mathematics*, vol. 15, pp. 137–151.

[4] P. R. Garabedian, "Oblique water entry of a wedge," *Communications on Pure and Applied Mathematics*, vol. 6, no. 2, pp. 157–165, 1953.

[5] P. R. Garabedian, "Asymptotic description of a free boundary at the point of separation," in *Applications of nonlinear partial differential equations in mathematical physics* (R. Finn, ed.), vol. XVII of *Proceedings of Symposia in Applied Mathematics*, (Providence, RI), p. 111, AMS, 1965.

[6] R. Cointe and J. L. Armand, "Hydrodynamic impact analysis of a cylinder," *Journal of Offshore Mechanics and Arctic Engineering*, vol. 109, pp. 237–243, 1987.

[7] S. D. Howison, J. R. Ockendon, and J. M. Oliver, "Oblique slamming, planing and skimming," *Journal of Engineering Mathematics*, vol. 48, pp. 321–337, 2004.

[8] A. A. Korobkin, "Analytical models of water impact," *European Journal of Applied Mathematics*, vol. 15, pp. 821–838, 2004.

[9] M. Greenhow, "Wedge entry into initially calm water," *Applied Ocean Research*, vol. 9, pp. 214–223, 1987.

[10] X. Mei, Y. Lui, and D. K. P. Yue, "On the water impact of general two-dimensional sections," *Applied Ocean Research*, vol. 21, pp. 1–15, 1999.

[11] E. Cumberbatch, "The impact of a water wedge on the wall," *Journal of Fluid Mechanics*, vol. 7, pp. 353–374, 1960.

[12] Z. N. Dobrovol'skaya, "Some problems of similarity flow of fluid with a free surface," *Journal of Fluid Mechanics*, vol. 36, pp. 805–829, 1969.

[13] R. Zhao and O. Faltinsen, "Water-entry of two-dimensional bodies," *Journal of Fluid Mechanics*, vol. 246, pp. 593–612, 1993.

[14] Y. A. Semenov and A. Iafrati, "On the nonlinear water entry problem of asymmetric wedges," *Journal of Fluid Mechanics*, vol. 547, pp. 231–256, 2006.

[15] Y. A. Semenov, G. X. Wu, and J. M. Oliver, "Splash jet caused by collision of two liquid wedges," *Journal of Fluid Mechanics*, vol. 737, pp. 132–145, 2013.

[16] A. Iafrati and A. A. Korobkin, "Initial stage of flat plate impact onto liquid free surface," *Physics of Fluids*, vol. 16, pp. 2214–2227, 2004.

[17] O. M. Faltinsen, *Hydrodynamics of high-speed marine vehicles*. Cambridge University Press, 2005.

[18] M. Shakeri, M. Tavakolinejad, and J. H. Duncan, "An experimental investigation of divergent bow waves simulated by a two-dimensional plus temporal wave marker technique," *Journal of Fluid Mechanics*, vol. 634, pp. 217–243, 2009.

[19] H. Climent, L. Benitez, F. Rueda, and N. Toso-Pentecote, "Aircraft ditching numerical simulation," in *ICAS 2006*, 2006.

[20] Y. A. Semenov and L. J. Cummings, "Free boundary Darcy flows with surface tension: Analytical and numerical study," *European Journal of Applied Mathematics*, vol. 17, pp. 607–631, 2006.

[21] N. E. Joukovskii, *Modification of Kirchhof's method for determination of a fluid motion in two directions at a fixed velocity given on the unknown streamline*, vol. XV of *Mathematical Transactions*. Moscow: Moscow Mathematical Society, 1890.

[22] J. H. Michell, "On the theory of free stream lines," *Philosophical Transactions of the Royal Society A*, vol. 181, pp. 389–431, 1890.

[23] M. I. Gurevich, *Theory of jets in ideal fluids*. New York: Academic Press, 1965.

[24] M. Brillouin, "Les surfaces de glissement de Helmholtz et la résistance des fluids," *Annales de Chimie et de Physique*, vol. 23, pp. 145–230, 1911.

[25] H. Villat, "Sur la validité des solutions de certains problèmes d'Hydrodynamique," *Journal de Mathématiques Pures et Appliquées*, vol. 10, pp. 231–290, 1914.

[26] Y. A. Semenov and G. X. Wu, "Water entry of an expanding wedge/plate with flow detachment," *Journal of Fluid Mechanics*, vol. 797, pp. 322–344.

[27] J. M. Oliver, "Second-order Wagner theory for two-dimensional water-entry problems at small deadrise angles," *Journal of Fluid Mechanics*, vol. 572, pp. 59–85, 2007.

***Ю. М. Савченко, Ю. А. Семенов, О. І. Наумова***

**Удар об воду циліндричного тіла, що розширюється**

На основі теорії потенціалу нестисливої швидкості теоретично вивчено автомодельний потік з бризковим струменем, який утворено внаслідок входу у воду двовимірного тіла довільної форми, що розширюється. Потік вважався безвихровим, а рідина — ідеальною, гравітація і поверхневий натяг не враховувались. Розв'язок отримано у вигляді інтегральних рівнянь з використанням інтегрального методу годографа. Показано, що розв'язок з від'єднаним бризковим струменем існує в усьому діапазоні швидкостей розширення від нуля до нескінченності. Представлено докладні результати з точки зору розподілу тиску, форми вільної поверхні й ліній течії, контактного кута бризкового струменя.

*КЛЮЧОВІ СЛОВА: вхід у воду, течія з вільною поверхнею, бризковий струмінь*

***Ю. Н. Савченко, Ю. А. Семенов, Е. И. Наумова***

**Удар о воду расширяющегося цилиндрического тела**

На основе теории потенциала несжимаемой скорости теоретически изучен автомодельный поток с брызговой струей, создаваемой входом в воду расширяющегося двумерного тела произвольной формы. Поток считался безвихревым, жидкость идеальная, гравитация и поверхностное натяжение не учитывались. Решение получено в виде интегральных уравнений с использованием интегрального метода годографа. Показано, что решение с отсоединенной брызговой струей существует во всем диапазоне расширения скоростей от нуля до бесконечности. Представлены подробные результаты с точки зрения распределения давления, формы свободной поверхности и линий тока, контактного угла брызговой струи.

*КЛЮЧЕВЫЕ СЛОВА: вход в воду, течение со свободной поверхностью, брызговая струя*